Received: 10 November 2023 | Revised: 17 May 2024 | Accepted: 30 May 2024

IET Communications

DOI: 10.1049/cmu2.12797

The Institution of Engineering and Technology WILEY

ORIGINAL RESEARCH

Noise modelling and mitigation for broadband in-door power line communication systems

Ogunlade M. Adegoke[1] | **Saheed Lekan Gbadamosi**[2,3] | **Babatunde S. Adejumobi**[1] | **Israel E. Owolabi**[1] | **Wasiu Adeyemi Oke**[4] | **Nnamdi I. Nwulu**[3]

[1]Department of Electrical, Electronic and Computer Engineering, Afe Babalola University, Ado-Ekiti, Ekiti, Nigeria

[2]Department of Electrical and Electronic Engineering, Bowen University, Iwo, Osun, Nigeria

[3]Center for Cyber Physical Food, Energy and Water Systems, University of Johannesburg, Auckland Park, Gauteng, South Africa

[4]Department of Mechanical and Mechatronics Engineering, Afe Babalola University, Ado, Ekiti, Nigeria

Correspondence
Saheed Lekan Gbadamosi, Department of Electrical and Electronic Engineering, Bowen University Iwo, Osun State, Nigeria.
Email: gbadamosiadeolu@gmail.com

Abstract

Communication systems are greatly hampered by many disruptive noises in powerline communication systems (PLC), which come with strong interference, resulting in the malfunction of PLC systems. Hence, there is a need to model noise and its effect on communication systems. This paper presents noise modelling and mitigation techniques for indoor broadband powerline communication systems. To model the PLC noise, frequency domain measurements employing the GSP-930 spectrum analyser were carried out to determine the noise frequency response in the frequency range of 1–30 MHz. The results obtained were plotted. While the analytical model for the noise model is presented, furthermore, noise mitigation techniques for multiple input multiple output PLC (MIMO-PLC) systems in the form of spatial modulation PLC systems have been proposed. The SM-PLC system employs the indices of the individual transmit lines to increase the data rate, as opposed to the traditional MIMO-PLC systems, where the symbol to be transmitted is transmitted by duplicating the symbol across all lines. The proposed system uses the maximum likelihood (ML) detector at the receiver to obtain estimates of the transmitted symbols. The simulation results of the SM-PLC system are compared with the already existing MIMO-PLC system and show a significant improvement of ≈6 dB and 5.2 dB in signal-to-noise ratio (SNR) at a bit error rate of 10(−5) for spectral efficiencies of 4 bits per channel use (bpcu) and 6 bpcu, respectively. On comparison of the SM-PLC system having a combination of additive white Gaussian noise and impulse noise at the receiver, the SM-PLC system outperformed the traditional MIMO-PLC by 3.5 and 3.8 dB in SNR for 4 and 6 bpcu, respectively.

1 | INTRODUCTION

Data transmission via electrical networks is made possible by power line communication technology [1], owing to the accessibility of power distribution systems even at remote locations, making PLC an avoidable communication solution. PLC in connection with the Internet of Things (IoT) are widely used for smart grid systems, increasing its popularity amongst data transmission systems. PLC uses the existing powerline infrastructure to transmit information together with electric current, and offers a solution with numerous benefits, such as affordability and extensive coverage. Similarly, it can also be found underground, under water, and in buildings with metal walls that have any link to radio signals [2, 3]. In recent years, several PLC-enabled applications have been implemented, such as narrowband (NB) PLCs with a frequency of 3–500 KHz, mostly used for automation and control purposes [3], broadband (BB) PLCs operating at a high frequency band of 2–30 MHz, which are used for residential internet connections and home/office local area networking. Despite several benefits to PLC, it is constantly constrained by noise interference along its route. This noise in the powerline is intrinsically complicated and is made up of a number of different elements, such as coloured background noise, narrowband noise, and impulsive noise [4, 5]. The PLC research is driven by these problems in order to increase capacity and communication range.

This is an open access article under the terms of the Creative Commons Attribution-NonCommercial License, which permits use, distribution and reproduction in any medium, provided the original work is properly cited and is not used for commercial purposes.
© 2024 The Author(s). *IET Communications* published by John Wiley & Sons Ltd on behalf of The Institution of Engineering and Technology.

The electromagnetic compatibility (EMC) and electromagnetic interference (EMI) of power networks both have an impact on broadband power line communication (BPL). Electrical wiring is vulnerable to radio frequency (RF) radiation from other radio services using the same band. Parts of the 1–30 MHz spectrum, where broadband PLC networks operate, are also used by amateur radio, amplitude modulation (AM), and frequency modulation (FM). The insulation provided by polyvinyl chloride (PVC) is more than adequate for the intended function, so it is obvious that the cable manufacturers are not responsible for providing shielding against any interference [3, 6]. Finding new strategies to reduce the consequences of narrowband interference will consequently continue to be a problem for PLC engineers and researchers [7]. Both academia and industrial partners are continually seeking ways to reduce the noise effect in PLC.

A survey of the literature shows that several works have been done to reduce noise effects on PLC. In [8], techniques for impulsive noise reduction in power line communication systems were carried out. Numerous methods, including forward error correction (FEC), interleavers, signal processing techniques, iterative suppression algorithms, compressed sensing (CS), and sparse Bayesian learning (SBL), have been suggested in this area to lessen the pronounced impacts of impulsive noise in PLC systems. Further study on impulsive noise mitigation, according to the authors, should focus on more reliable detection and estimation methods, using specialized non-linear filters, CS and SBL, and combinations of FEC algorithms. Subcarrier rotation and symbol rotation techniques were two methods for increasing the data rate of PLC systems that were reported in [2]. Depending on the approach, the approaches can boost the data rate while efficiently reducing the PLC's impulse noise and additive white Gaussian noise (AWGN). According to the authors [9], measurements and analyses have been done to determine the effects of various noise types on the power line communications (PLC) channel. The noise has been mitigated using adaptive noise canceller (ANC) and the least mean square (LMS) filter method. Both impulsive and Gaussian noise can be effectively cancelled with the LMS filter. According to simulation data, the LMS filter reduces the bit error rate (BER). Also, the operation of the power line carrier (PLC) system, its features, and how it enables the transmission of power and information were all covered in [10]. It explains the various components' step-by-step functions and how they enable information dispersion. Future directions for improvements in the power line carrier system were also discussed. Challenges were also considered, and solutions were offered. A number of methods to deal with PLC noise while employing MIMO transmission have been proposed, thereby serving as the PLC transmission strategy [3].

The performance of the PLC system's indoor channel is examined [11], and the authors detect various types of noise in the channel. Variations in frequency, duration, and line-to-line variability are observed in the power-line channel noise. The author categorizes various noise types, describes their traits, and explains how to remove them from power line channels. Among them are coloured and background noise. The additive white Gaussian noise (AWGN) and the coloured noise model are comparable. Long-term measurements were conducted from 1 to 30 MHz in order to characterize the background noise characteristics of the PLC channel. The Nakagami-m distribution function is similar to the probability distribution of the time domain noise amplitude. Additionally, impulsive noises are investigated at their sources using a novel approach. When compared to noise measurements at the receiver side, measuring noise at the source allowed for far less noise analysis and the establishment of an effective correction for device noise generators. It was feasible to suggest an impulsive noise model for any electrical equipment by characterizing noise at the source. In [12], the authors provided a summary of impulse noise and related models in addition to highlighting some noteworthy and fascinating details about the field that are occasionally disregarded or poorly understood. The noise models are classified as having memory (Markov–Middleton and Markov–Gaussian) and without having memory (Middleton Class A and Bernoulli–Gaussian). The authors also examine the Middleton Class A model's five-term approximation of the probability density function (PDF). It demonstrated how the Middleton Class A model and the Bernoulli–Gaussian model are comparable and can be used interchangeably. The authors also covered the symmetric alpha (α)-stable distribution that is used to simulate impulse noise, in addition to the Middleton Class A and Bernoulli–Gaussian models. A comparison was made between the PDFs of the Middleton Classes A and B. The PDFs for all three models showed fat tails. Bernoulli–Gaussian models and the symmetric alpha (α)-stable distribution as an impulse noise model. Additionally, contrast the bit error rate performance of communications systems operating under impulsive noise, such as single-carrier (SC) and multi-carrier (MC) systems. The results showed that single-carrier modulation performs better than multi-carrier modulation under low probability of impulse noise occurrence. Recently, the effects of pulse jamming in PLC over log-normal channel gain with Gaussian–Gaussian additive noise have been considered [13]. The impact of a random pulse jamming attack on PLC systems, assuming log-normally distributed channel gain over M-Ary phase shift keying (M-PSL), is examined by the author. The Bernoulli–Gaussian random process describes the nature of PLC channel noise. Furthermore, the Bernoulli random variables describe the jammer's state. The differential chaos shift keying (DCSK), correlated chaos shift keying (CDSK), and differential sequence differential phase shift keying (DS-DPSK) modulation schemes are outperformed by the suggested M-ary phase shift keying (M-PSK) modulation-based PLC system. The Middleton canonical class A distribution's usefulness for modelling the noise amplitude in narrowband power line communications (NB-PLC) is examined by the author [14]. Based on the Kolmogorov–Smirnov test, only 14.47% (45 out of 311) of the observed registers can be modelled with the class A distribution, suggesting that the distribution's capacity to represent the measured noise is somewhat limited. This decreased capacity is mostly caused by the class A PDF's sharp peak and fat tail shapes, which do not fit over the shoulders of the majority of empirical PDFs. The impulsive index and the Gaussian to impulsive power noise ratio have been demonstrated to have an inverse relationship, and in 80% of the cases, the infinite sum in the class A PDF can be shortened to four terms. Moreover, in 56%

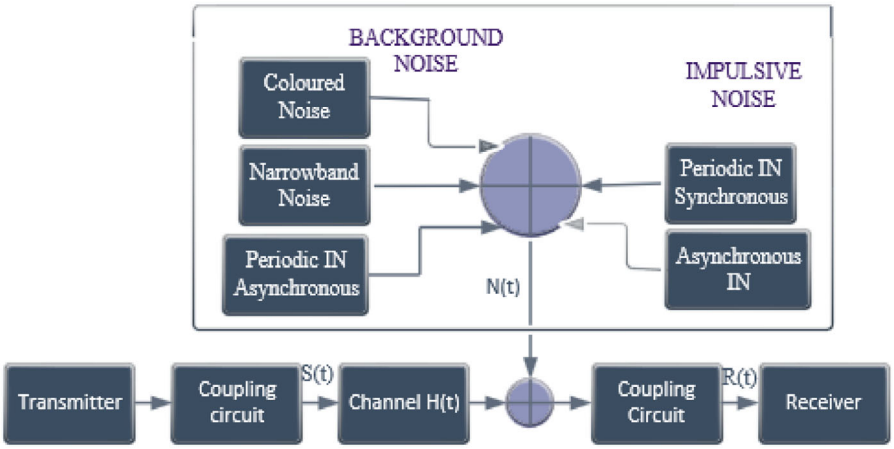

FIGURE 1 Classes of noise in PLC [7, 17].

of the cases, two terms are sufficient, suggesting that the more straightforward Bernoulli–Gaussian model can be applied in an identical manner. Using multiple impulsive distributions, author [15], presents comparative research on modelling the impulsive noise amplitude in indoor PLC systems. The impulsive noise model for PLC systems frequently used in the literature is the Middleton Class A distribution. Other distribution families that were considered were the symmetric α-Stable (SαS), generalized Gaussian, Bernoulli Gaussian, Student's *t*, and Middleton Gaussian. The simulation studies look into real indoor PLC system noise measurements, and the results demonstrate that, when compared to the other families, the SαS distribution achieves the best modelling success in terms of the statistical error criteria, particularly for the tail characteristics of the measured data sets. Five potential statistical models were compared in order to model the impulsive noise for indoor PLC systems. The outcomes proved that the SαS distribution performed better than the others, and they also showed that the SαS distribution is a good fit for modelling PLC impulsive noise. Despite being widely used; the study's findings indicate that the Middleton Class A model is not the best option and can only represent a limited amount of impulsiveness in indoor PLC measures through experimentation. Furthermore, the purpose of this work is to compare the BER performances of the proposed SM-PLC system and the conventional MIMO-PLC system, in which all symbols are concurrently sent over multiple lines. Furthermore, the comparison between the AWGN SM-PLC system and the MIMO-PLC with AWGN uses the introduction of impulse noise using multiplication factors of 1.1, 1.3, 1.5, 1.7, and 2. The comparison is necessary because it is anticipated that MIMO-PLC will perform better than SM-PLC if the performance of the two systems is comparable. But that is not the case.

2 | CLASSIFICATION OF NOISE IN PLC

One of the key features influencing communication performance through the channel is noise in PLC systems. The sources of noise that are widely available in the PLC channel are AWGN, frequency selective fading, impulse noise, and frequency disturbance [16]. To effectively utilize power lines for a reliable high-speed data transmission system, it is essential to study and understand the various noise scenarios present in the PLC network. These systems are frequently disrupted by noise generated by both internal and external equipment connected to or located near the power line transmission network. The regular usage of electrical equipment and appliances inevitably results in interference. Every electrical outlet generates noise, in addition to the ambient noise produced by all the appliances connected to the electrical circuit. According to [4, 7, 17], noise can be categorized into two namely, background noise and impulsive noise. The background noise can be divided into narrowband noise, impulsive noise (IN) and coloured background noise, while the impulsive noise can be classified as periodic synchronous impulsive noise and asynchronous impulsive noise, as shown in Figure 1. A PLC channel is defined by its channel transfer function H(t), which the transmitted signal S(t) traverses. Prior to reaching the receiver R(t), various forms of noise are introduced [7, 18, 19].

3 | MEASUREMENT TECHNIQUES

The noise measurements were carried out in the frequency domain. Signal generator, coupling circuit, and spectrum analyser are a few of the tools utilized for the noise measurements. The frequency domain measurement was performed using the spectrum analyser GSP- 930. The spectrum analyser GWInstek GSP-930, is a new-generation platform-based 3 GHz. It has a model number GSP-930, with frequency range of 9KHz–3 GHz. The brand is GWInstek. This is being done to determine the noise frequency response in the frequency range of 1–30 MHz [17, 19]. The frequency band for a broadband power line communication system extends from 1 to 30 MHz, and a signal generator is utilized to inject the frequencies of interest into the power line. One of the most important pieces of equipment in electronics and communication is the signal

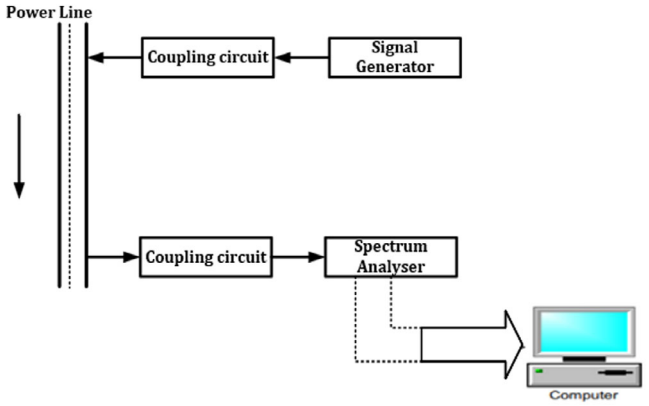

FIGURE 2 Block diagram for PLC noise measurement.

FIGURE 3 Experimental set up.

TABLE 1 Classes of broadband indoor PLC loads.

Capacitive loads	Inductive loads	Resistive loads
Cables	Television	Lamp
Radio circuits	Speakers	Heaters
Fluorescent Light	Air condition	Heating coil
Phone charger	Laptop	Soldering Iron
Laptop charger	Refrigerator	Electric iron
Capacitor bank	Washing machine	Electric kettle
Television Picture tube	Fans	Rice cooker

generator. For a range of tasks like testing, debugging, and designing, it is utilized to generate various signals and frequencies. The key components of frequency specifications are resolution, switching speed, accuracy, and range. The spectrum analyser offers an extremely low noise floor, great frequency stability, and a number of instruments for adjusting the sweep range. To get the display trace, it records and saves the measured data to an external storage device. The mathematical operations that were performed in order to produce traces from the measured data were specified by the trace setting. The universal serial bus (USB) ports on the analyser, which are used to connect external storage devices for additional processing and analysis outside the device, were utilized to access the stored data [17, 19]. Also, an AC coupling circuit (Steval-XPLMOICPL) power line communication was used primarily to disconnect the measuring instruments from the AC supply. It is manufactured by STMicroelectronics. It acts as an interface between the PLC channel and the measurement equipment. Galvanic isolation between measurement equipment and the mains is provided by the coupling circuit, which also makes it easier to receive specific noise signals. It can be used to inject a signal from an arbitrary function signal generator (LODESTAR signal generator brand, manufactured in Taiwan) and for laboratory tools like a spectrum analyzer. "It allows the frequency of interest to get through while blocking the power line's 50 Hz AC frequency [17, 19]. Figure 2 depicts the block representation of PLC noise measurement. The details of the experimental set up is shown in Figure 3.

The broadband indoor measured loads are resistive, capacitive and inductive loads as depicted in Table 1.

4 | NOISE MODELLING ANALYSIS

Drawing a smooth curve through the data may sometimes be the main goal rather than extracting or interpreting fitted parameters. Nonparametric fitting is the term used to describe this process. One of the various nonparametric fitting techniques is the smoothing spline. The curve must be changed from a least-squares straight-line approximation to a cubic spline interpolant in order to change the degree of smoothness. A smoothing spline or another smoothing technique, such as moving average filtering, Savitzky–Golay filtering, or local regression smoothing, can be used to match the noisy data. To approximate associations between a predictor x_i and an observation y_i, smoothing splines are a fantastic tool. The goal of smoothing splines is to identify a function that can minimize among all other possible functions [20].

$$\sum_{i}^{n} \{y_i - \emptyset(x_i)\}^2 + \beta \int \{\emptyset^n(t)\}^2 \, dt, \propto \geq 0. \tag{1}$$

The function $\emptyset$ that minimizes Equation (1) is referred to as a smoothing function while β is a positive tuning parameter. The first and second terms in Equation (1) are the loss function and penalty term, also known as the roughness penalty, according to [21]. The loss function supports $\emptyset$ to fit the data well while the penalty term penalizes the inconsistency in $\emptyset$. As an alternative, this second term supports $\emptyset$ to be smooth and the larger the value of β, the smoother the $\emptyset$. It is crucial to understand that when $\beta = 0$, the penalty term has no impact and accordingly, the $\emptyset$ will precisely interpolate the training observations. Also, $\emptyset$ will be completely smooth when $\beta \to \infty$ and it will just be a straight line that passes as intimately as achievable to the training points. That is, $\emptyset$ will be the linear least squares line. However, $\emptyset$ will approximate the training observations but will be fairly smooth when β is $0 < \beta < \infty$. The function that minimizes Equation (1) has a few exceptional properties that include: It is a piecewise cubic polynomial with knots at the distinctive values of, and the first and second derivatives are continuous at each

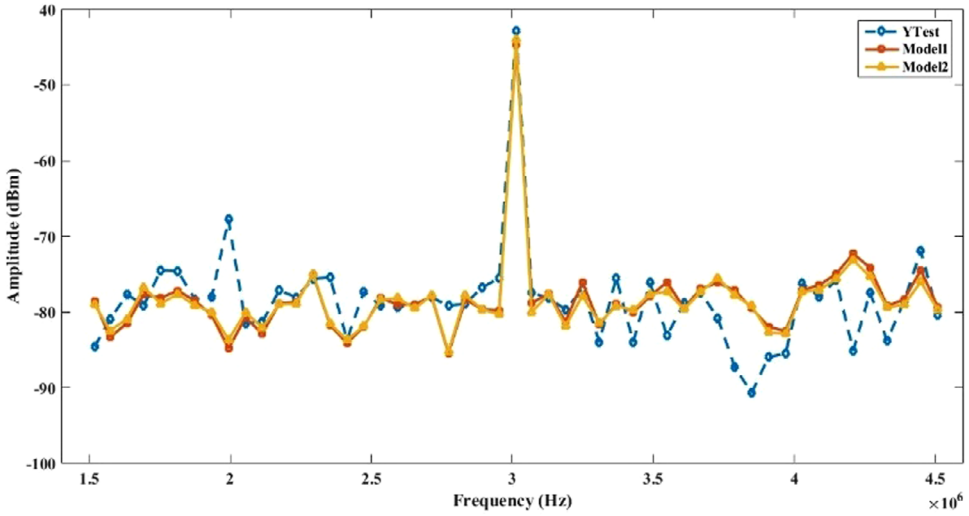

FIGURE 4 Results obtained when models were tested with data from 3 MHz frequency.

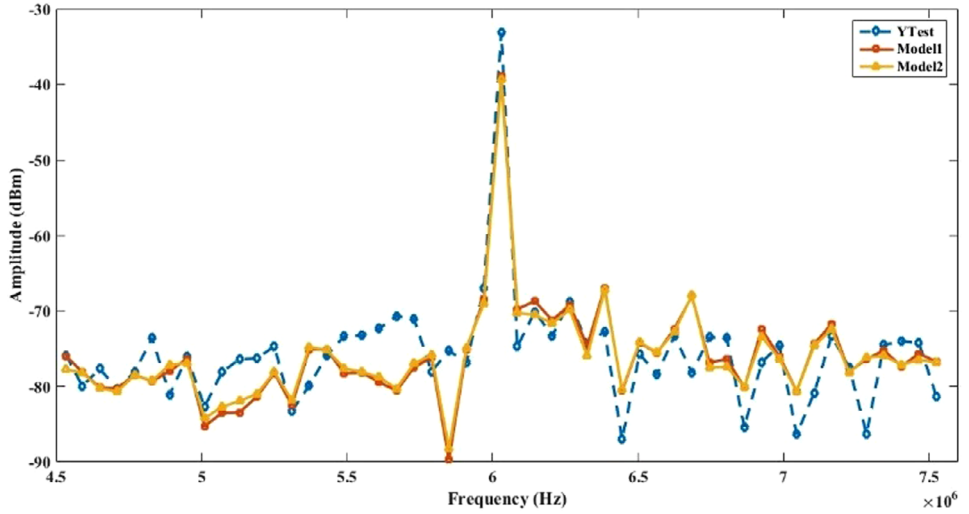

FIGURE 5 Results obtained when models were tested with data from 6 MHz frequency.

knot. For the specified smoothing parameter $\propto$ and the specified weight w_i the smoothing spline $\emptyset$ and it minimizes [20].

$$\propto \sum_i w_i\{y_i - \emptyset(x_i)\}^2 + (1-\propto)\int \{\emptyset^n(x)\}^2 dx \qquad (2)$$

The weights in Equation (2) are normally assumed to be 1 for all data points if they are not stated while $\propto$ is a value between 0 and 1. Besides, a least-squares straight-line fit to the data will be generated if $\propto = 0$ while a cubic spline interpolant will be produced when $\propto = 1$. Hence, the entire Equation (2) will be involved during minimization when, $0 < \propto < 1$. This equation is implemented in MATLAB for smoothing splines and the value of $\propto$ will be selected automatically, in the "interesting range" if it is not stated. Figures 3–12 show the models and corresponding amplitudes that were observed in the frequency range of 3–30 MHz. The noise waveform exhibits different characteristics, and equations were developed. The goodness fit criterion, or how well the equation represents the data points, is measured by four different factors. The factors are root mean square (RMSE), the sum of squares due to error (SSE), adjusted *R*-square, and *R*-square. The SSE simply shows the sum of squares of the deviations of the measured data values from the predicted values. It evaluates how well the independent variable fitted the data. On the other hand, *R*-square is a metric for assessing how well a model fits the data and explains its variation. It is regarded as the square of the correlation between the response values and the predicted response values. However, the better the fit, the higher the *R*-square value. Where *R*-square has a value between 0 and 1. The adjusted *R*-square is a normalizing variation of the *R*-square caused by negligible independent variables. The root mean squared error is a statistic that is also referred to as the fit standard error and the regression

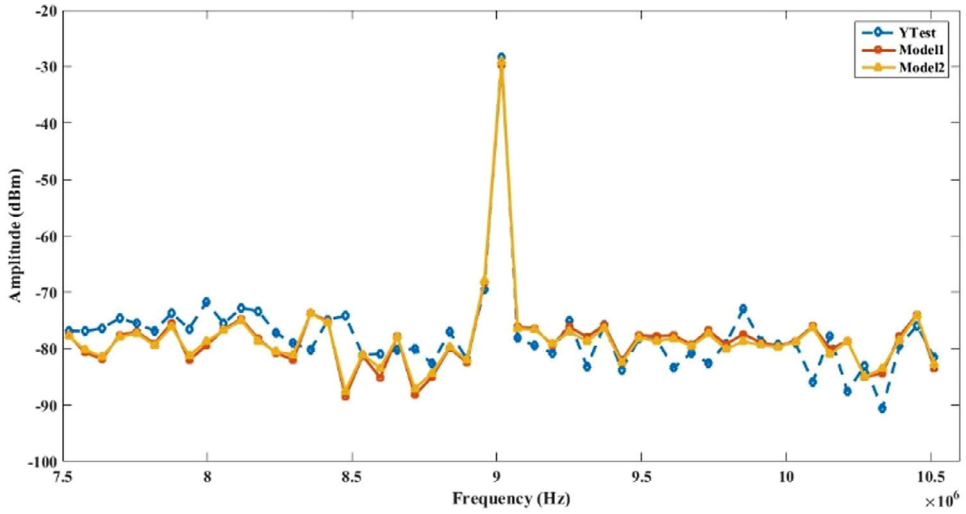

FIGURE 6 Results obtained when models were tested with data from 9 MHz frequency.

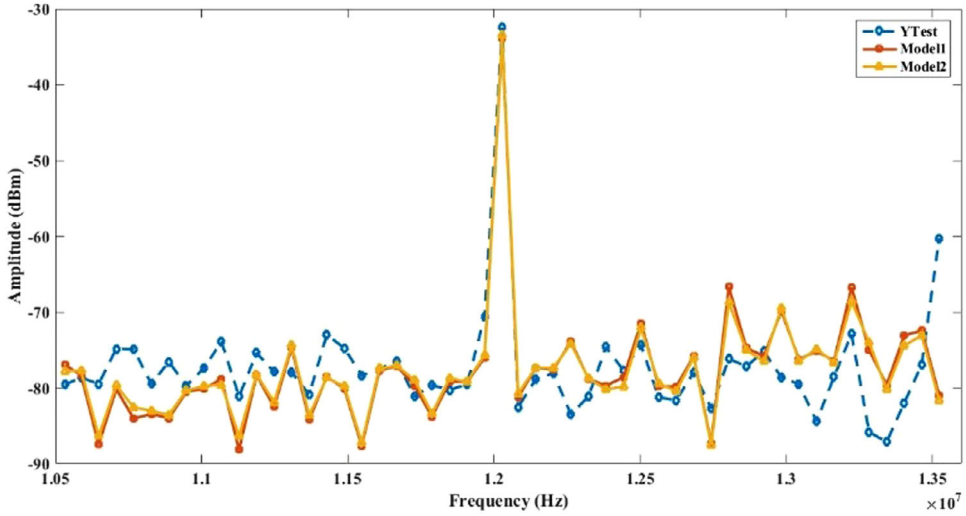

FIGURE 7 Results obtained when models were tested with data from 12 MHz frequency.

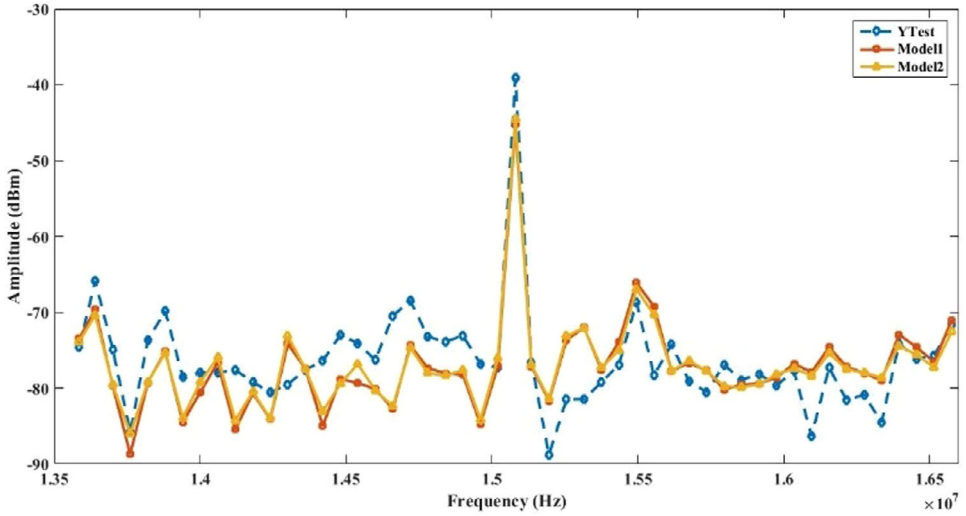

FIGURE 8 Results obtained when models were tested with data from 15 MHz frequency.

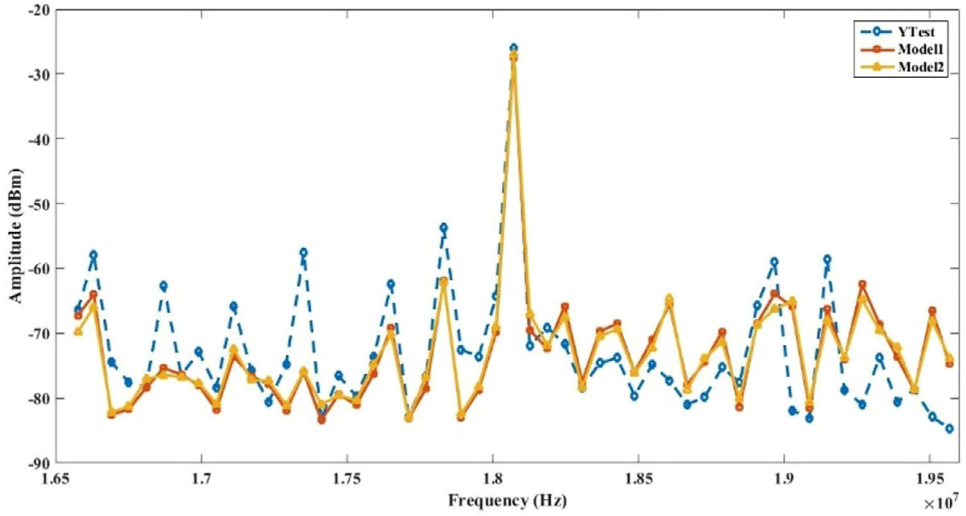

FIGURE 9 Results obtained when models were tested with data from 18 MHz frequency.

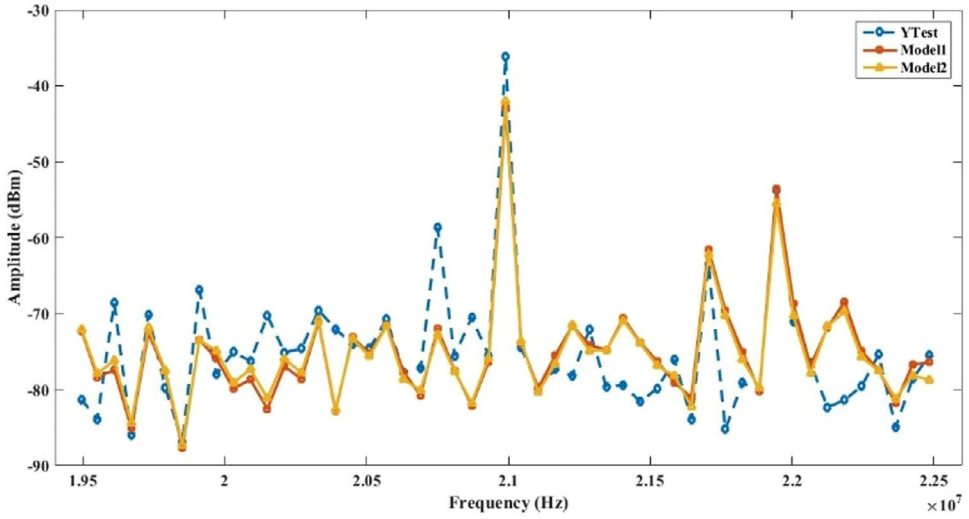

FIGURE 10 Results obtained when models were tested with data from 21 MHz frequency.

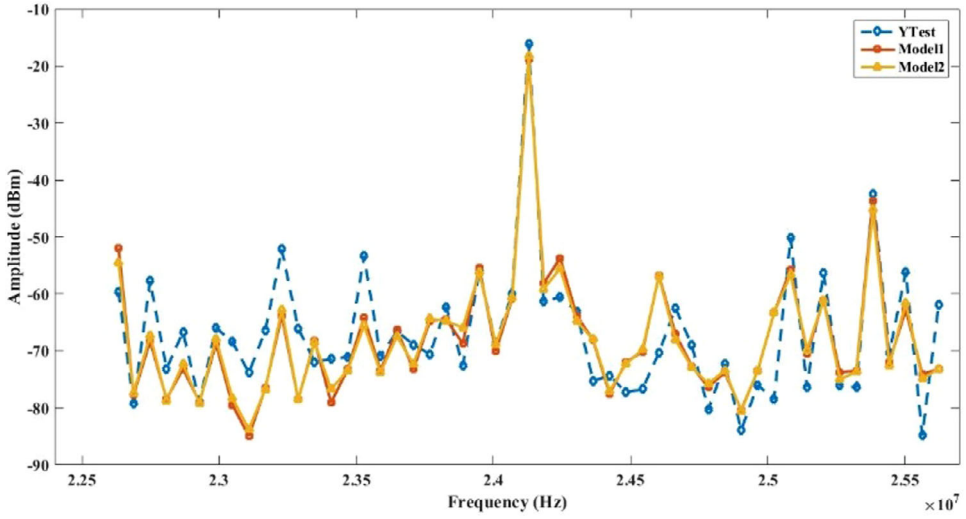

FIGURE 11 Results obtained when models were tested with data from 24 MHz frequency.

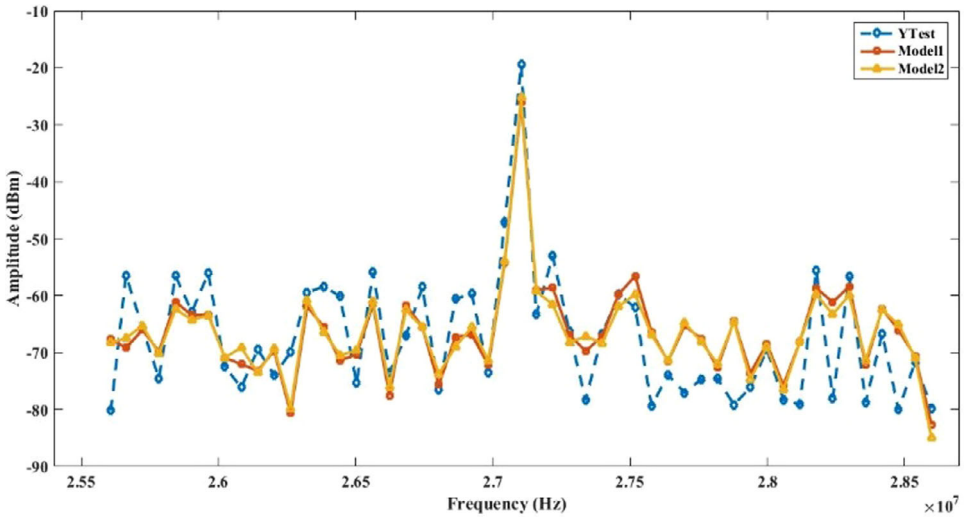

FIGURE 12 Results obtained when models were tested with data from 27 MHz frequency.

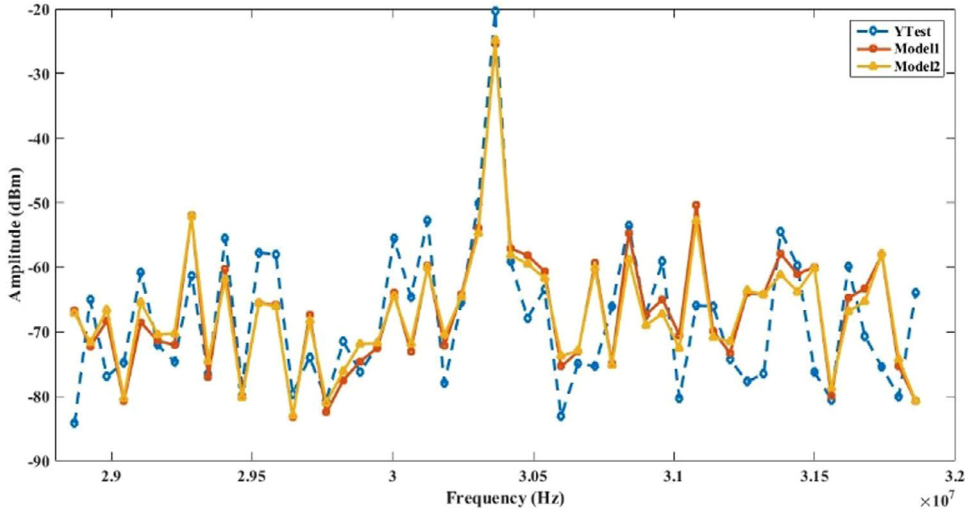

FIGURE 13 Results obtained when models were tested with data from 30 MHz frequency.

standard error. It is a projection of the random component of the data's standard deviation. The models obtained for 3–30 MHz are shown in Figures 4–13.

Y-Test: The actual/expected results.

Spline_1: Results obtained when the first model was considered.

Spline_2: Results obtained when the second model was considered.

5 | SYSTEM MODEL FOR NOISE MITIGATION TECHNIQUES

The system model of the proposed noise mitigation technique is presented in Figure 14.

The input bits of a PLC system that are to be transmitted through the PLC channel are divided into two groups of bits. A group is used to select a symbol from an M-Ary QAM constellation, while the second group of bits is employed to select the transmit line from the L available lines. Hence, the spectral efficiency for the SM-PLC system for a single subcarrier may be represented as [22]:

$$S_{\mathrm{SM-PLC}} = \log_2 M + \log_2 L \tag{3}$$

where M is the constellation size of the M-ary quadrature amplitude and/or phase modulation (M QAM) and L is the number of transmit power lines. However, for the traditional MIMO-PLC system, where the symbols to be transmitted is broadcast via all the power lines, the spectral efficiency may be represented as [22]:

$$S_{\mathrm{MIMO-PLC}} = \log_2 M \tag{4}$$

The next step entails the conversion of the bits to indexes such that the indexes determine the transmit symbol and transmit lines as presented in Table 2. An example of the bit

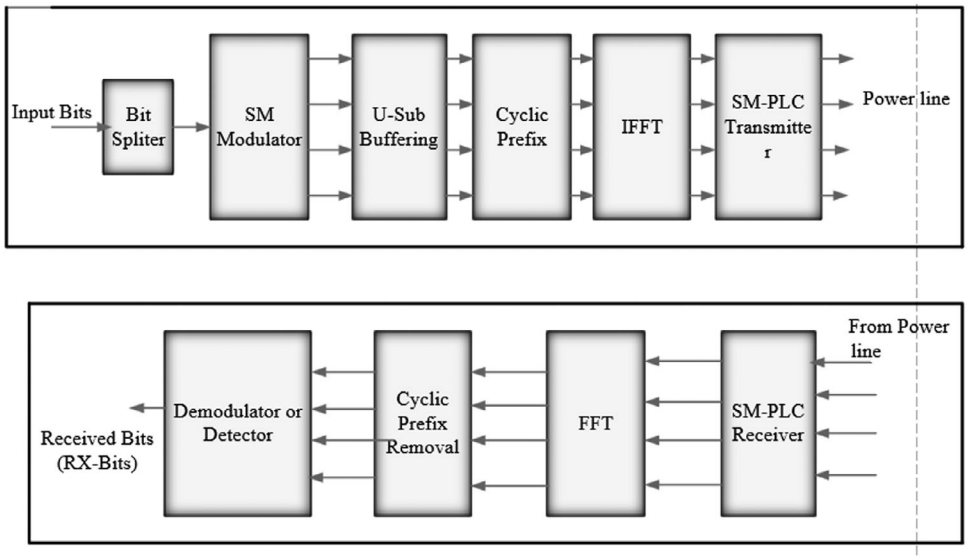

FIGURE 14 System models for noise mitigation techniques.

TABLE 2 Bit assignment technique for SM-PLC with 4-QAM and 4-lines.

Input bits	Symbol bits	Line bits	Symbol index	Line index	4-QAM
0000	00	00	1	1	S_1
0100	01	00	2	1	S_2
0110	10	10	2	3	S_3
1111	11	11	4	4	S_4
1010	10	10	3	3	S_3
1001	10	10	3	2	S_3

TABLE 3 Bit assignment technique for 16-QAM and 4-lines SM-PLC system.

Input bits	Symbol bits	Line bits	Symbol index	Line index	16-QAM
000000	0000	00	1	1	S_1
010111	0101	11	6	4	S_6
111101	1111	01	16	2	S_{16}
111111	1111	11	16	4	S_{16}
101011	1010	11	11	4	S_{11}
110110	1101	10	14	2	S_{10}

assignment for an SM-PLC system which makes use of four lines and 4-QAM constellation is given in Table 2.

The outputs from the SM-PLC modulator are then mapped into an $L \times 1$ vector having the ℓ-th element, for $\ell \in [1 : L]$ as the only non-zero item in the vector.

Given a 4-QAM constellation having its symbols as $[s_1\ s_2\ s_3\ s_4]$, if it is assumed that four lines are used for the transmission. The outputs of the SM-PLC system given in Table 3 are as presented in Table 4.

TABLE 4 Shows subcarrier transmit vector.

Symbol index	Line index	Subcarrier vector
1	1	$[S_1\ 0\ 0\ 0]^T$
2	1	$[S_2\ 0\ 0\ 0]^T$
2	3	$[0\ 0\ S_2\ 0]^T$
3	2	$[0\ S_2\ 0\ 0]^T$
1	4	$[0\ 0\ 0\ S_1]^T$

The output from the spatial modulator is stacked to obtain a matrix Z given as:

$$Z_{a,b} = \begin{bmatrix} Z_{1,1} & Z_{1,2} & \cdots & Z_{1,U} \\ Z_{2,1} & Z_{2,2} & \cdots & Z_{2,U} \\ \vdots & \vdots & \ddots & \vdots \\ Z_{L,1} & Z_{L,2} & \cdots & Z_{L,U} \end{bmatrix} \tag{5}$$

where $Z_{a,b}$ is the frequency domain element for the a-th line and the b-th subcarrier. L and U represent the number of power lines and the number of usable subcarriers, respectively.

The SM-PLC system makes use of cyclic prefix having a cyclic prefix length of C. Hence, the matrix in (5) may be rewritten as:

$$Z = \begin{bmatrix} Z_{1,1} & \cdots & Z_{1,C} & \cdots & Z_{1,U} \\ Z_{2,1} & \cdots & Z_{2,C} & \cdots & Z_{2,U} \\ \vdots & \cdots & \vdots & \ddots & \vdots \\ Z_{L,1} & \cdots & Z_{L,C} & \cdots & Z_{L,U} \end{bmatrix} \tag{6}$$

The $L \times C$ matric of Z is used to perform cyclic prefixing on the Z matrix to obtain a new matrix Z_{new} which is an $L \times N_{fft}$

matrix given as:

$$Z_{new} = \begin{bmatrix} Z_{1,1} & \cdots & Z_{1,C} & \cdots & Z_{1,U} & Z_{1,1} & \cdots & Z_{1,C} \\ Z_{2,1} & \cdots & Z_{2,C} & \cdots & Z_{2,U} & Z_{2,1} & \cdots & Z_{2,C} \\ \vdots & \cdots & \vdots & \vdots & \vdots & \vdots & \ddots & \vdots \\ Z_{L,1} & \cdots & Z_{L,C} & \cdots & Z_{L,U} & Z_{L,1} & \cdots & Z_{L,C} \end{bmatrix} \tag{7}$$

Therefore, Z_{new} may be rewritten as:

$$\boldsymbol{Z} = \begin{bmatrix} Z_{1,1} & Z_{1,2} & \cdots & Z_{1,N_{fft}} \\ Z_{2,1} & Z_{2,2} & \cdots & Z_{2,N_{fft}} \\ \vdots & \vdots & \ddots & \vdots \\ Z_{L,1} & Z_{L,2} & \cdots & Z_{L,N_{fft}} \end{bmatrix} \tag{8}$$

where N_{fft} is equal to the sum of U and C.

To obtain the time domain signals of Z, the Inverse FFT (IFFT) is performed on Z and is represented by the function given as [2, 22]:

$$U_{lk}(t) = \sum_{k=0}^{N_{fft}-1} Z_{lk} e^{j2\pi \frac{kt}{T}} \tag{9}$$

where $U_{lk}(t)$ is the time domain sub carrier value for the l-th, for $l \in [1:L]$ line and the k-th, for $k \in [1:N_{fft}]$ subcarrier. Z_{lk} is the k-th item in the $\boldsymbol{Z}$ matrix to be transmitted on the l-th line. T is the period of one OFDM symbol, and t is time slice for one subcarrier. N_{fft} is the IFFT size. The time domain received signal of the transmitted SM-PLC system can be represented as [22]:

$$\boldsymbol{Y} = \sqrt{p}\,\boldsymbol{Z} + \boldsymbol{N} \tag{10}$$

where $\boldsymbol{N}$ is the broadband noise obtained from the indoor broadband noise modelled as shown in Equation (2).

The FFT transformation is performed on the received signal to obtain the frequency domain signal. The FFT of the received signal is given as [2, 22]:

$$U_{lk}(t) = \frac{1}{\sqrt{N_{fft}}} \sum_{k=0}^{N_{fft}-1} X_{lk} e^{\frac{j2\pi k}{N_{fft}}} \tag{11}$$

To obtain the transmitted symbols, the maximum likelihood (ML) detection is performed on the received signal given as [22]:

$$[\hat{a}\ \hat{s}] = \underset{\substack{a \in [1:L],\ b \in [1:U], \\ s \in [1:M]}}{\operatorname{argmin}} \left(\| Y_p - Z_p \|_F^2 \right) \tag{12}$$

where Y_p is the p-th column vector, for $p \in [1:U]$ of the received signal after performing the FFT and the cyclic prefix is removed. $\hat{a}$ and $\hat{s}$ are the a-th and s-th detected lines and symbols, respectively. F is the Frobenius norm.

6 | RESULTS AND DISCUSSION

The data used was obtained from ten frequency ranges (3, 6, 9…, 30), with each range having size data termed F-dat. The size data was selected randomly from each F-dat and labelled Test-dat. The size data, referred to as FitValdat, then remained for fitting and validation. The titles of the three columns in each data set include S/N, frequency (Hz), and amplitude (dBm). During the fitting, 97.8% of FitValdat was used, while the remaining was utilized for validation. Several fits were produced, but most of the fits generated results that were not significantly different from each other when validated. Consequently, two fits were selected randomly from them. The R-square and adjusted R-square of the selected fits are obtained to show their qualities. It should be remembered that R-square statistics are normally employed to decide the best fit, and it can be any value between 0 and 1, with a value closer to 1 signifying a better fit [21]. Also, the adjusted R-square statistic is normally the best pointer of the fit quality when extra coefficients are added to the fit. Its value can be any value less than or equal to 1, with a value closer to 1 signifying a better fit. The R-square and adjusted R-square of the selected fits are presented in Table 5, while the predicted results for the selected fits when tested with Testdat for each frequency range compared with expected results (Y-test) are shown in Figures 4–13 (for 3 MHz) to 10 (for 30 MHz). It can be observed in all figures that the predicted results followed the expected results.

In this section, the simulation results for 4-bit SM-PLC and 4-bit MIMO PLC are compared for AWGN and a combination of AWGN and impulse noise in the form of A-impulse noise. Likewise, the simulation comparing the results for AWGN and A-impulse noise for 6 bpcu SM-PLC and 6 bpcu MIMO PLC is presented. The introduction of impulse noise using varying multiplying factors of the AWGN noise power for the impulse noise $\rho = 1.1, 1.3, 1.5, 1.7$ and 2 to the AWGN SM-PLC system is compared with MIMO-PLC having AWGN. The reason for this comparison is that, if the schemes have superior performance, it is expected that MIMO-PLC would outperform SM-PLC.

Considering Figure 15, it depicts the results for the spectral efficiencies of 4 and 6 bpcu of the proposed system in comparison with the traditional MIMO-PLC system with AWGN at the receiver. The proposed 4 bpcu SM-PLC system employs 4 lines with an M-Ary QAM of 4 QAM, while the MIMO-PLC system employs only the 16QAM for the modulation without cognizance of the number of power lines. The constellation size for the modulation is usually higher for MIMO-PLC because

TABLE 5 Model properties.

Model/Fit no.	Smoothing parameters	R square	Adjusted R square
1	$1.5e^{-10}$	0.95681	0.84422
2	0.35678	1	1

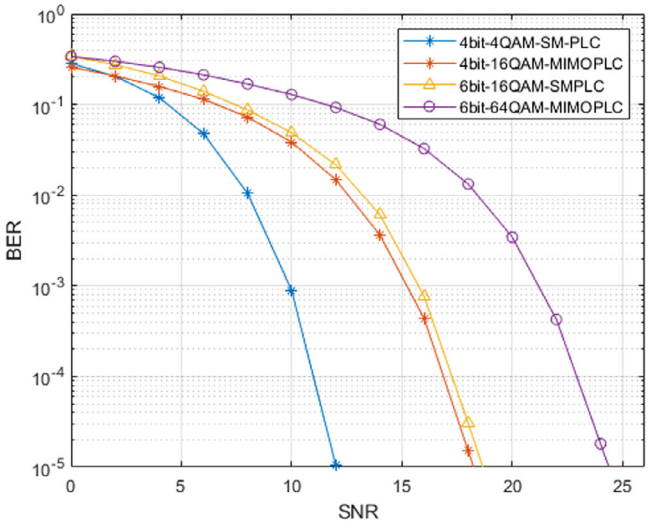

FIGURE 15 BER performance for MIMO-PLC and SM-PLC for 4 and 6 bpcu with AWGN at the receiver.

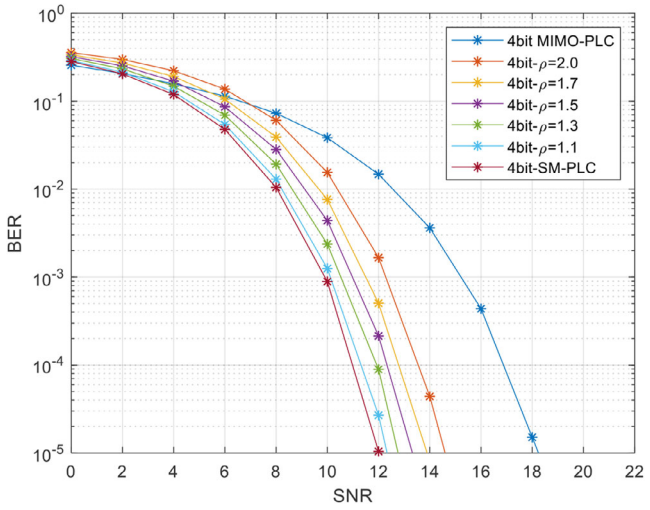

FIGURE 16 Comparison of 4 bpcu AWGN-based SM-PLC and MIMO-PLC system with A-impulse SM-PLC.

the number of power lines being employed is inconsequential to the number of bits being transmitted. In the case of the 6 bpcu SM-PLC system, the SM-PLC system employs four lines with an M-Ary QAM of 16 QAM. However, the 6 bpcu MIMO-PLC system makes use of 64QAM for the modulation. Considering the proposed 4 bpcu SM-PLC system in comparison with the 4 bpcu MIMO-PLC system, it can be noted that, the proposed system outperforms the MIMO-PLC system with a gain in SNR of $\approx$ 6 dB when the BER is 10^{-5}. However, when the 6 bpcu of both systems is compared for the same BER (10^{-5}), the gain in SNR by the SM-PLC system over the MIMO-PLC is $\approx$ 5.2 dB.

Figure 16 presents the results of the comparison between the proposed SM-PLC system and the conventional MIMO-PLC system, where all the symbols are transmitted simultaneously by utilizing multiple lines. Furthermore, different spike values in terms of the impulse noise power in combination with the

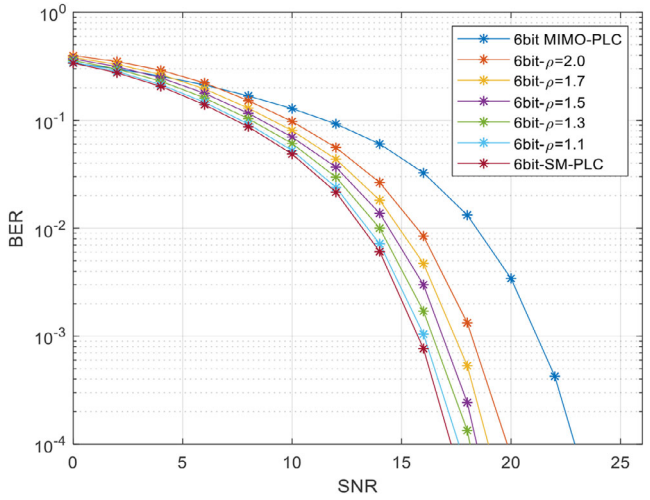

FIGURE 17 Comparison of 6 bpcu AWGN-based SM-PLC and MIMO-PLC system with A-impulse SM-PLC.

AWGN (A-impulse noise) on the SM-PLC system are compared with MIMO-PLC and SM-PLC systems over AWGN for a 4 bpcu. As seen in Figure 16, the SM-PLC system for both AWGN and A-impulse noise showed improved performance over the MIMO-PLC system. For example, at a BER of 10^{-5}, the AWGN and A-impulse SM-PLC system outperforms the MIMO-PLC system by a minimum gain of $\approx$ 3.5 dB in SNR. However, this is not so, as the SM-PLC having impulse noise of twice the power of AWGN showed a more improved performance of approximately $\approx$ 3.5 dB gain in SNR over the MIMO PLC system at a BER of 10^{-5}. The different values of ρ like 1.1 and 1.7 presented a better performance than the MIMO-PLC system.

In a similar comparison, Figures 16 and 17 present the results for a 6 bpcu system for AWGN-based SM-PLC and MIMO-PLC systems in comparison with SM-PLC with A-impulse noise. As seen in Figure 16, the SM-PLC system with AWGN showed improved performance over the MIMO-PLC system. For example, at a BER of 10^{-4}, the SM-PLC system outperformed the AWGN-based MIMO-PLC system by a gain of 6.5 dB in SNR. Furthermore, the introduction of A-impulse noise using varying multiplying factors $\rho = 1.1$, 1.3, 1.5, 1.7 and 2 to the SM-PLC system is compared with the AWGN-based MIMO-PLC. The reason for comparison is that if the schemes have similar performance, it is expected that MIMO-PLC should outperform SM-PLC because of the spikes introduced by the impulse noise. However, this is not so, as the A-impulse SM-PLC having $\rho = 2$ showed a more improved performance of approximately $\approx$ 3.8 dB gain in SNR over the MIMO-PLC system at a BER of 10^{-4}. Lower values of ρ like 1.1 and 1.7 presented even better performance than $\rho = 2$.

In order to investigate the behaviour of the proposed SM-PLC system in relation to the channel effects, we consider an M-QAM SM-PLC system under the influence of log-normal fading channel and additive white gaussian noise which may be represented as [23]:

$$\boldsymbol{y} = \boldsymbol{h}x + \boldsymbol{n} \tag{13}$$

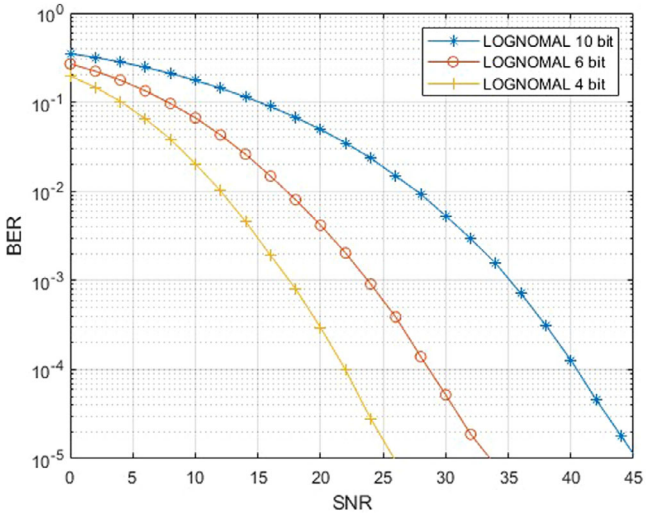

FIGURE 18 BER performance for SM-PLC over lognormal fading channel. The performances of the different spectral efficiencies.

As described in [23], the channel fading coefficient h is a log-normal distributed random variable having a probability density function defined as:

$$f_H(h) = \frac{1}{h\sqrt{2\pi\sigma_h^2}} exp^{\frac{(\ln h - \mu_h)^2}{2\sigma_h^2}} \quad (14)$$

For the purpose of simulation, the defined log-normal channel given in [23], with a variance $\sigma_h = 1$ dB is considered, while the noise follows the Gaussian distribution with $C(0, 1)$. Furthermore, we assume a perfect correlation between the channels. The simulated result for the system given in Equation (13), is presented by the plots in Figure 18.

From the plots given in Figure 18, the power needed to achieve a given BER performance is seen to increase with the increase in spectral efficiency. For example, as expected, to achieve a BER of 10^{-5}, when the spectral efficiency is increased from 4 to 6 bpcu, an increase in power of ≈ 7 dB will be required. In a similar manner, for an increase from 6 to 10 bpcu, an increase in power by 12 dB is required to attain a BER performance of 10^{-5}.

7 | CONCLUSION

When the AWGN is introduced and all symbols are sent utilizing multiple lines simultaneously, the BER performances of the conventional MIMO PLC system and the suggested SM-PLC system are compared. By gaining 6 dB in SNR, the SM-PLC system outperformed the MIMO-PLC system in terms of performance. Furthermore, the SM-PLC system is compared with MIMO-PLC, having AWGN by adding impulse noise to the AWGN using varying factors of 1.1, 1.3, 1.5, 1.7, and 2. The comparison is necessary because it is anticipated that MIMO-PLC will perform better than SM-PLC if the two methods have comparable performance. This is untrue, though, as the SM-PLC, which has impulse noise twice as strong as AWGN, has shown significantly better performance than the MIMO PLC system at a BER of 10^{-5} with a gain in SNR of about 3.5 dB. Even better performance was shown by values of 1.1 and 1.7 than by = 2. Finally, when compared to the MIMO-PLC system, the SM-PLC system performed better.

In order to investigate the behaviour of the proposed SM-PLC system in relation to the channel effects, we consider an M.

8 | FUTURE WORK

To further expand the research on SM-PLC systems, the effects of channel correction need to be investigated.

AUTHOR CONTRIBUTIONS

Ogunlade M. Adegoke: Data curation; formal analysis; investigation; methodology; resources; software; visualization; writing—original draft. **Saheed Lekan Gbadamosi**: Conceptualization; formal analysis; investigation; methodology; project administration; resources; supervision; validation; visualization; writing—review and editing. **Babatunde S. Adejumobi**: Formal analysis; investigation; methodology; software; validation; writing—review and editing. **Israel E. Owolabi**: Conceptualization; project administration; resources; supervision; writing—review and editing. **Wasiu Adeyemi Oke**: Data curation; formal analysis; software; validation. **Nnamdi I. Nwulu**: Conceptualization; project administration; resources; supervision; writing—review and editing.

CONFLICT OF INTEREST STATEMENT

The authors declare no conflicts of interest.

DATA AVAILABILITY STATEMENT

The data will be made available on request due to privacy and ethical restrictions.

ORCID

Saheed Lekan Gbadamosi https://orcid.org/0000-0001-7398-8134

REFERENCES

1. Laksir, S., Chaoub, A., Tamtaoui, A.: Impulsive noise reduction techniques in power line communication: A survey and recent trends. In: Proceedings of the 2018 International Workshop on Technologies, Algorithms, Models, Platforms and Applications for Smart Cities, pp. 13–19. IEEE, Piscataway, NJ (2018). https://doi.org/10.1504/IJAACS.2019.098607
2. Adejumobi, B.S., Shongwe, T., Hasan, A.N.: Improved subcarrier selection technique for power line communications. J. Commun. 18(2), 123–128 (2023). https://doi.org/10.12720/jcm.18.2.123-128
3. Cheng, X., Cao, R., Yang, L.: Relay-aided amplify-and-forward powerline communications. IEEE Trans. Smart Grid 4(1), 265–272 (2013). https://doi.org/10.1109/TSG.2012.2225645
4. Nyete, A.M.: A flexible statistical frame work for the characterization and modelling of noise in powerline communication channels. Dissertation, University of Kwazulu-Natal (2015)
5. Oyeleke, O.D., Idowu-Bismark, O., Andrew, A., Dyaji, C.B., Muhammad, I., Adamu, T.: Noise characterization and modelling for powerline

communications in Nigeria. In: Proceedings of the IEEE International Conference on Computational Intelligence and Virtual Environments for Measurement Systems and Applications—CIVEMSA 2021, pp. 2–7. IEEE, Piscataway, NJ (2021). https://doi.org/10.1109/CIVEMSA52099.2021.9493668
6. Ndolo, A., Çavdar, İ.H.: Current state of communication systems based on electrical power transmission lines. J. Electr. Syst. Inf. Technol. 8, 1–10 (2021). https://doi.org/10.1186/s43067-021-00028-9
7. Mosalaosi, M.: Power line communication (PLC) channel measurements and charaterization. Dissertation, University of Kwazulu-Natal (2014)
8. Laksir, S., Chaoub, A., Tamtaoui, A.: Impulsive noise reduction techniques in power line communication: A survey. Int. J. Auton. Adapt. Commun. Syst. 12(2), 146–186 (2019). https://doi.org/10.1504/IJAACS.2019.098607
9. Rajkumarsingh, B., Sokappadu, B.N.: Noise Mitigation in a Power Line Communication Channel, pp. 180–191. Springer, Berlin, Heidelberg (2019). https://doi.org/10.1007/978-3-030-18240-3_17
10. Amuta, E.O., Awelewa, A., Olajube, A., Somefun, T.E., Afolabi, G., Uyi, A.S.: Power line carrier technologies: A review. IOP Conf. Ser.: Mater. Sci. Eng. 1036, 012062 (2021). https://doi.org/10.1088/1757-899x/1036/1/012062
11. Shrotriya, A., Saxena, D.K., Singh, M.K.: Noise in power line communication channel: An overview. Int. J. Eng. Res. Dev. 9(2), 1–5 (2013)
12. Shongwe, T., Vinck, A.J.H., Ferreira, H.C.: A study on impulse noise and its models. Trans. South Afr. Inst. Electr. Eng. 106(3), 119–131 (2015)
13. Mohan, V., Mathur, A.: Pulse jamming in PLC over log-normal channel gain with Bernoulli-Gaussian additive noise. IEEE Commun. Lett. 27(10), 2603–2607 (2023). https://doi.org/10.1109/LCOMM.2023.3301063
14. Cortes, J.A., Sanz, A., Estopinan, P., Garcia, J.I.: On the suitability of the Middleton class: A noise model for narrowband PLC. In: Proceedings of the International Symposium on Power Line Communications and its Applications, ISPLC 2016, pp. 58–63. IEEE, Piscataway, NJ (2016). https://doi.org/10.1109/ISPLC.2016.7476256
15. Karakuş, O., Kuruoğlu, E.E., Altınkaya, M.A.: Modelling impulsive noise in indoor powerline communication systems. Signal, Image Video Process. 14(8), 1655–1661 (2020). https://doi.org/10.1007/s11760-020-01708-1
16. Papilaya, V.N., Shongwe, T., Vinck, A.J.H., Ferreira, H.C.: Selected subcarriers QPSK-OFDM transmission schemes to combat frequency disturbances. In: Proceedings of the 2012 IEEE International Symposium on Power Line Communications and Its Applications, pp. 202–204. IEEE, Piscataway, NJ (2012). https://doi.org/10.1109/ISPLC.2012.6201327
17. Ogunlade, M.A., Gbadamosui, S.L., Owolabi, I.E., Nwulu, N.I.: Noise measurement, characterization, and modeling for broadband indoor power communication system: A comprehensive survey. Energies 16(1535), 17–18 (2023)
18. Meng, H., Guan, Y.L., Chen, S.: Modeling and analysis of noise effects on broadband power-line communications. IEEE Trans. Power Delivery 20(2), 630–632 (2005). https://doi.org/10.1109/TPWRD.2005.844349
19. Ogunlade, A.O., Adegoke, M., Banjo, I.O.: In-home power line frequency domain noise measurement and analysis for broadband communication. ARPN J. Eng. Appl. Sci. 16(17), 1825–1826 (2021)
20. Curve Fitting ToolboxTM: User's Guide. MATLAB Manual, pp. 7–200. papers2://publication/uuid/1AB1E427-49D2-43BA-BE5C-B64EE88F3947 (2011). Accessed 10 October 2023
21. Hastie, T., Tibshirani, R., James, G., Witten, D.: An Introduction to Statistical Learning. vol. 102, Springer, Berlin (2023)
22. Adejumobi, B.S., Pillay, N.: Quadrature spatial modulation orthogonal frequency division multiplexing. J. Telecommun. Electron. Comput. Eng. 10(4), 51–53 (2018)
23. Jani, M., Garg, P., Bansal, A.: Performance analysis of a PLC system over log-normal fading channel and impulsive noise. In: Proceedings of the International Conference on Computing and Network Communications (CoCoNet), pp. 480–484. IEEE, Piscataway, NJ (2016). https://doi.org/10.1109/CoCoNet.2015.7411229

How to cite this article: Adegoke, O.M., Gbadamosi, S.L., Adejumobi, B.S., Owolabi, I.E., Oke, W.A., Nwulu, N.I.: Noise modelling and mitigation for broadband in-door power line communication systems. IET Commun. 18, 869–881 (2024). https://doi.org/10.1049/cmu2.12797